Lunar University Network for Astrophysics Research

MEMO SERIES

MEMO A-6

Field Tests of a Polyimide Film Antenna Conducted November 2010

E. Polisensky, K. Stewart, B. Hicks, K. Weiler

(Naval Research Laboratory)

Field Tests of a Polyimide Film Antenna Conducted November 2010

E. Polisensky, K. Stewart, B. Hicks, K. Weiler (NRL)
8 September 2011

We report on field tests of a polyimide thin-film antenna deployed 12-14 November 2010 in a Maryland suburb outside Washington, DC (39° N latitude). The dipole antenna consisted of a 5 μm thick copper layer deposited on a 25 μm thick Kapton film. Each dipole arm was 8 m long and 30.5 cm wide. The inner 1 m of each arm was tapered to a point where a 1:1 wideband passive balun was attached. Coaxial cable connected the balun to an RFSpace SDR-14 software-defined receiver. The antenna was laid directly on the ground and held in place with clothespins (Figure 1).

Figure 1: The polyimide film antenna as deployed. The antenna was tested on moist, grass-covered soil.

Observations

The receiver recorded a spectrum from 0-30 MHz every 10 minutes for approximately 50 continuous hours in channels of 1.017 kHz bandwidth. Figure 2 shows the received power as a function of Local Sidereal Time (LST) and frequency. The data are not calibrated and no corrections for cable, balun, ground, or reflection losses have been included.

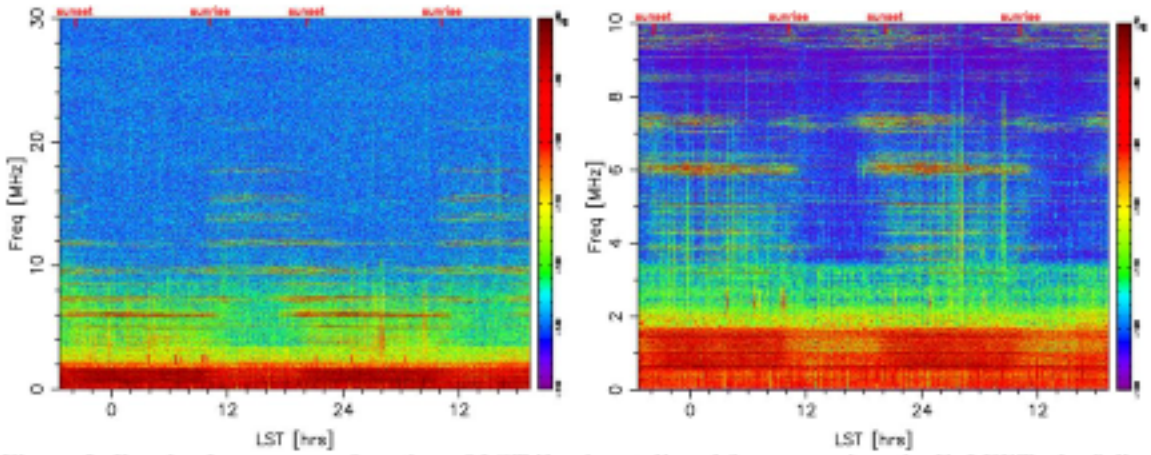

Figure 2: Received power as a function of LST [horizontal] and frequency [vertical]. LEFT: the full 0-30 MHz band. RIGHT: 0-10 MHz emphasizing the low frequency absorption observed between sunrise and sunset.

Local noon occurred at LST ~ 15 hrs and a decrease in power below ~ 7 MHz centered on this time is evident. This feature is examined further in Figure 3 which shows the power as a function of time for frequency bands at 1, 4, and 6 MHz. These plots show a daytime drop in power that is broader at lower frequencies as would be expected from an increasing/decreasing electron density approaching sunrise/sunset due to absorption of terrestrial signals by the D layer of the ionosphere.

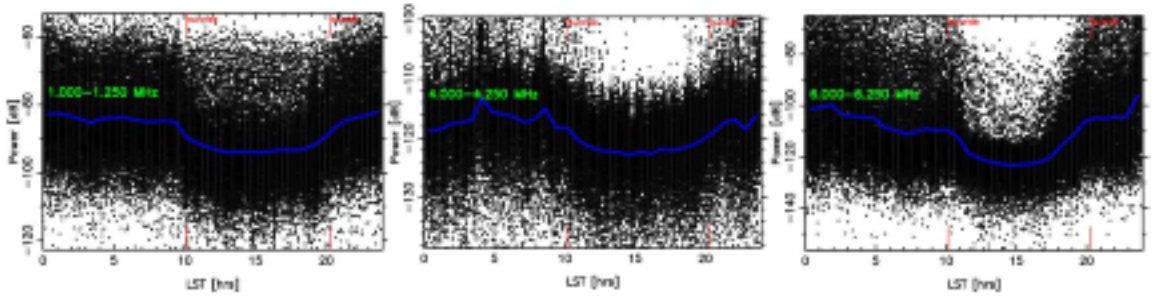

Figure 3: Power as a function of time for 3 frequency bands. The raw data is plotted in black and the average power binned in time is plotted in blue. Local sunrise and sunset times are marked in red.

Antenna Simulation

In numerical simulations of the antenna performance the dielectric constant and conductivity of the soil beneath the antenna were adjusted to give the best fit to the measured feedpoint impedance. The best-fit values were $\varepsilon = 8$ and $\sigma = 2.5$ mS/m. Figure 4 is a slice through the E-plane of the antenna pattern at 10 MHz and shows the response is nearly uniform over the sky hemisphere but with low gain, -13.5 dB, compared to an ideal isotropic antenna. The results are similar for the H-plane and for frequencies 10-30 MHz.

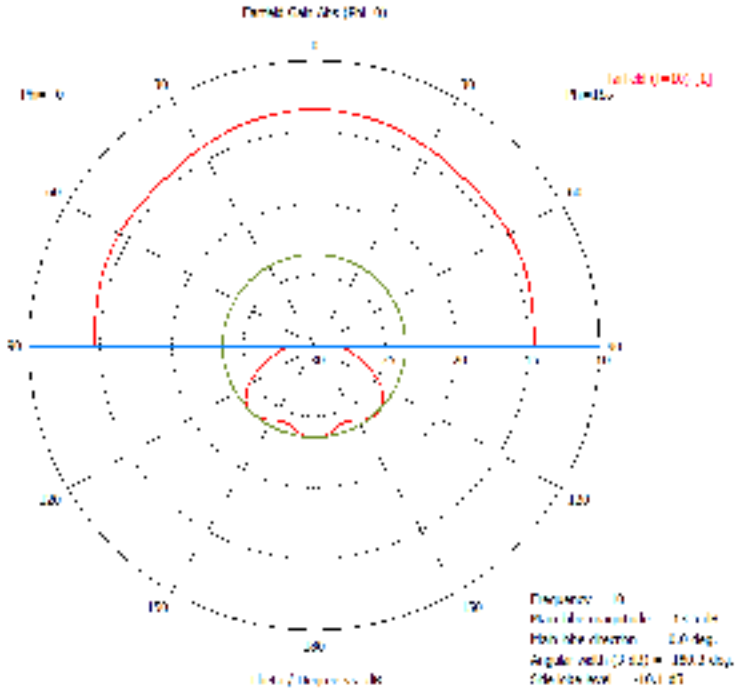

Figure 4 – Simulated farfield gain of the polyimide film antenna at 10 MHz. The antenna is nearly isotropic over the sky but with low gain due to the lossy ground.

Receiver Temperature

The receiver used for these measurements was an RFSpace SDR-14. Figure 5 shows a plot of the receiver noise figure from the manufacturer's web page (www.rfspace.com). The noise figure is related to the temperature by:

$$\mathbf{T = (F-1)\ T_0}$$

Where: T = receiver temperature
F = noise figure
T_0 = 290 K

From the noise figure plot the receiver temperature is estimated to be 3200 K below 23 MHz and 3600 K above.

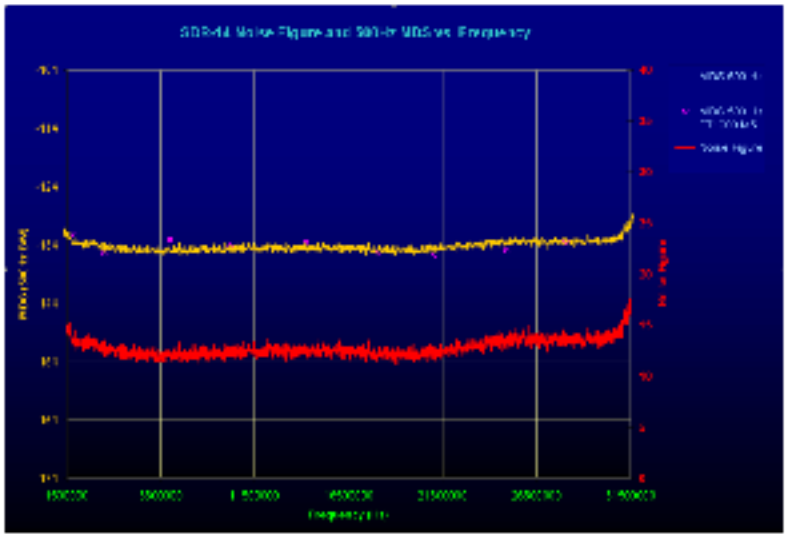

Figure 5 – Noise figure (red) for the SDR-14 receiver from the manufacturer's web site. The noise figure transitions from a value of about 12 to about 13.5 at 23 MHz. (The yellow curve is not relevant to the discussion here)

Drift Scans - Simulations

Simulations of the antenna temperature as a function of LST were conducted using sky maps generated with the Global Sky Map software of de Oliveira-Costa et al. (2008) and assuming an isotropic antenna with unit gain. Table 1 gives the maximum and minimum antenna temperatures and their ratio for several frequencies from 10-30 MHz. The diurnal variations have amplitudes of about 1.9 dB in the ideal case where the receiver temperature is negligible and the dominant signal is the Galactic background.
The expected temperature of the polyimide film antenna is similar to the isotropic antenna but scaled by the gain of the polyimide antenna, $G_{ANT} = 10^{-1.35} = 0.0447$, and combined with the receiver temperature. The last column of Table 1 gives the expected diurnal amplitude accounting for the antenna gain and the receiver temperature but assuming a perfect impedance match and lossless feedline. The variations are stronger at lower frequencies where the sky is brighter.

Table 1 – Results of drift scan simulations for an isotropic antenna

Freq [MHz]	T_{max} [K]	T_{min} [K]	T_{max}/T_{min} [dB]	$\frac{G_{ANT}T_{max} - T_{RX}}{G_{ANT}T_{min} + T_{RX}}$ [dB]
10	393765	254277	1.90	1.55
15	137248	88304	1.92	1.16
20	66782	42811	1.93	0.83
25	39295	25092	1.95	0.55
30	25907	16480	1.96	0.40

Drift Scans - Observations

The antenna data were examined and drift scans were plotted for channels that appeared to be free of transmitters and strong RFI. Figure 6 shows drift scan plots for 288 channels at frequencies 12.220-12.365 MHz and 12.403-12.550 MHz. The data were binned and averaged in LST and plotted in blue. Strong intermittent RFI, abundant during the daytime (left panel), were excised from the average power calculation by excluding data above -117 dB. The antenna temperatures from the drift scan simulations, accounting for the simulated antenna gain and the receiver temperature, were offset to the average observed power and plotted in pink.

From the right panel the data appear to show a diurnal variation with an amplitude comparable to the simulation, but the variation appears to be correlated more with the times of sunrise and sunset than the time of Galactic Center transit. Although we excised the strongest RFI, it is possible higher levels of daytime RFI due to increased propagation effects from the F-layer of the ionosphere are partially or wholly the cause of the rise in the average power level.

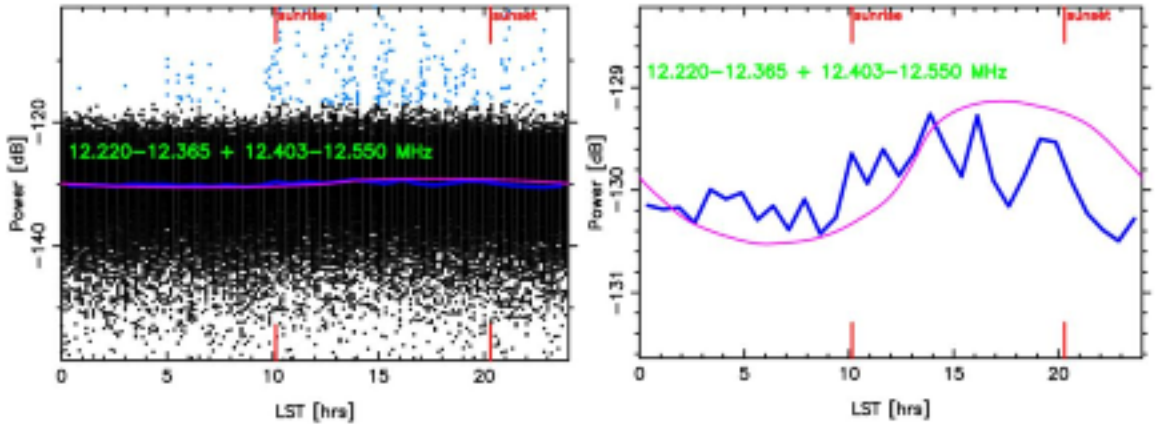

Figure 6: Drift scans for 288 channels in 2 select frequency bands. The raw data are plotted in black, the binned average in dark blue, and the simulation in pink. Strong RFI (blue points, left panel) were excluded from the calculation of the average power. There appears to be a diurnal variation in the average antenna power (right panel) but not conclusively due to the Galactic background.

Drift scans for frequency bands from 10-15 MHz show a diurnal variation similar to the one in Figure 6 but none are clearly due to the Galactic background. No diurnal variations are seen above 15 MHz but the signal amplitude may be small compared to the noise due to unaccounted for losses.

Future Prospects

The conclusion of this work is that no diurnal variations due to the Galactic background were conclusively observed at any frequency with the polyimide film antenna during the observation period. One problem is the low gain of the antenna due to the moist, lossy, ground conditions. Repeating the observations over dry ground or with the antenna

elevated will increase the gain. Simulations of the antenna response for different ground conditions can be used to predict the improvement. Table 2 shows the simulated amplitudes for several values of the antenna gain. Simulations using ground parameters for lunar regolith from the Apollo Lunar Sourcebook predict the gain of the antenna would be -11.4 to -13.5 dB from 5 to 20 MHz.

Table 2 – Simulated ($G_{ANT}T_{max} + T_{RX} / G_{ANT}T_{min} + T_{RX}$) [dB] for various values of the antenna gain, G_{ANT}.

G_{ANT}: Freq [MHz]	-18 dB	-16 dB	-14 dB	-12 dB	-10 dB
10	1.16	1.35	1.51	1.64	1.72
15	0.68	0.89	1.11	1.31	1.48
20	0.41	0.57	0.77	0.99	1.21
25	0.24	0.35	0.50	0.69	0.91
30	0.16	0.25	0.37	0.52	0.72

The amplitudes of diurnal variations are limited to a maximum of 1.9 dB at this latitude due to the nearly isotropic response of the antenna over the sky. This could potentially be improved by moving the antenna to a location where the sky contrast is greater over the course of a day. Drift scan simulations were run for frequencies from 10 to 30 MHz in 1° latitude steps for the Earth and Moon, see Figure 7. For the lunar simulations a Moon-centered equatorial coordinate system was created for the sky maps by rotating the Earth-centered coordinate system to account for the different orientation of the lunar spin axis relative to the Earth's (the coordinates of the lunar north celestial pole were obtained from Davies et al. (1996) and are currently: RA= 274°, Dec= 66°).

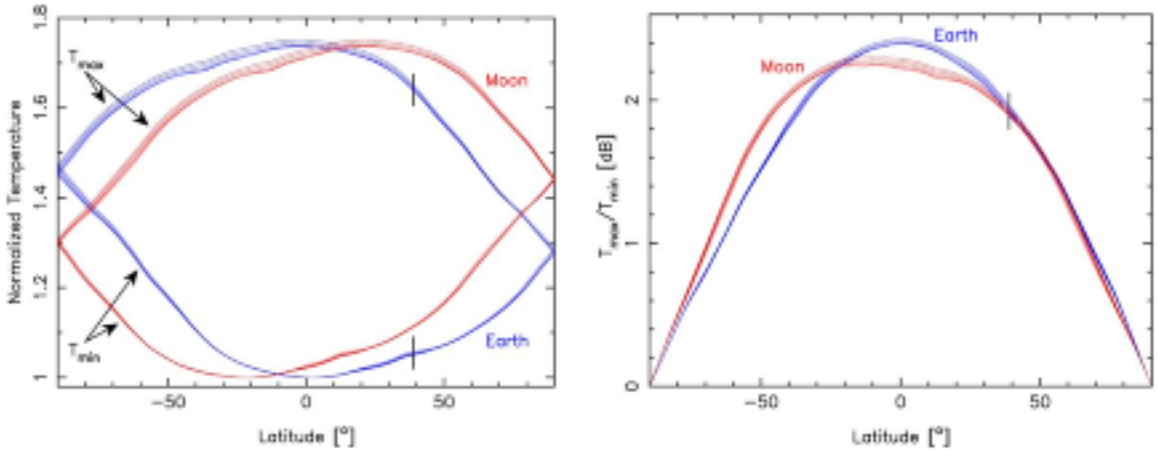

Figure 7: LEFT: Simulations from 10-30 MHz of T_{min} (lower curves) and T_{max} (upper curves) for an isotropic antenna as a function of latitude for the Earth (blue) and Moon (red). Temperatures have been normalized by the minimum value of T_{min} for all latitudes. The minimum value of T_{min} is nearly identical for the Earth and the Moon. RIGHT: The amplitude T_{max}/T_{min} for the data in the left panel. The short vertical lines indicate the latitude of our observations.

Figure 7 shows that, on the Earth, the amplitudes of diurnal variation increases as the isotropic antenna is moved toward the equator where it reaches a maximum of 2.4 dB. On the lunar surface the amplitudes reach a slightly lower peak of 2.2 dB but the peak is wider with a preference for the southern lunar latitudes. However, T_{min} is larger at northern lunar latitudes implying it is generally easier to achieve Galactic noise dominance for an isotropic antenna in the northern lunar hemisphere. Both of these features of the lunar simulations are due to the higher declination of the Galactic Center in the Moon-centered equatorial coordinate system (-5°) compared to the Earth-centered system (-27°).

Summary

We deployed a polyimide film antenna directly on grass-covered soil and recorded over 2 days of data. Broadband drift scans from 1 to 30 MHz indicate that the antenna was not sensitive enough to conclusively observe the diurnal variation of the Galactic background emission due to losses in the moist, clay soil, however variations in ionospheric propagation of MF and HF broadcast stations were observed.

We conducted simulations of the antenna that show the response is nearly isotropic over the sky but with low gain. Using maps of the Galactic background emission we also conducted multi-frequency simulations of the expected diurnal variations and explored the effects of the antenna gain on the amplitude of variations as well as the dependence on latitude for deployments on the Earth and the Moon.

Further field testing at a location with soil parameters closer to the lunar surface, e.g. very dry desert, would be useful since the diurnal amplitude will be greater and observable over a wider frequency band. Observations at several different times of year would help to separate ionospheric effects from the Galactic synchrotron radiation. Our observations of diurnal terrestrial ionospheric absorption illustrate how the polyimide film antenna might enable studies of the lunar ionosphere.

References

M.E. Davies et al., "Report of the IAU/IAG/COSPAR Working Group on Cartographic Coordinates and Rotational Elements of the Planets and Satellites: 1994," Celestial Mechanics and Dynamical Astronomy, 63, 127, 1996

de Oliveira-Costa et al.,"A model of diffuse Galactic radio emission from 10 MHz to 100 GHz," MNRAS, 388, 247, 2008